Silicon (2022) 14:5191–5206
https://doi.org/10.1007/s12633-021-01264-4

ORIGINAL PAPER

Enhanced Performance of Hydrogen Peroxide Modified Pozzolan-Based Geopolymer for Abatement of Methylene Blue from Aqueous Medium

Dzoujo T. Hermann[1] · Sylvain Tome[1] · Victor O. Shikuku[2] · Jean B. Tchuigwa[1] · Alex Spieß[3] · Christoph Janiak[3] · Marie Annie Etoh[1] · David Daniel Joh Dina[1]

Received: 11 May 2021 / Accepted: 4 July 2021 / Published online: 10 August 2021

Abstract
Pozzolan-based eco-adsorbents were synthesized by geopolymerization with addition of hydrogen peroxide (H_2O_2) with mass ratios 0% (GP_0) and 1% (GP_1) and the products used to sorb cationic methylene blue (MB) dye from water. The chemical composition, textural properties, mineral composition, surface functional groups, as well as morphology and internal structure of these samples were determined by the X-ray fluorescence, adsorption of nitrogen by the B.E.T (Bruamer Emmet Teller) method, X-ray diffraction, Fourier Transformed Infrared Spectroscopy (FTIR) and scanning electron microscopy (SEM), respectively. The effects of contact time, dye initial concentration, adsorbent dosage, pH and temperature were examined and are herein reported. Incorporation of 1% H_2O_2 increased the specific surface area from 4.344 to 5.610 m^2/g representing ~29% increase in surface area. This translated to an increase in the MB adsorption capacity by 15 orders of magnitude from 24.4 to 366.2 mg/g for GP_0 and GP_1, respectively. The adsorption rates of methylene blue onto the two geopolymers were best described by the pseudo-second order kinetic model. The adsorption equilibrium data were best described by the Sips and Freundlich isotherms models for GP_0 and GP_1, respectively. Thermodynamically, it was determined that the adsorption of methylene blue onto GP_0 and GP_1 is a physical and endothermic process. The results show that incorporation of a low amount of hydrogen peroxide into pozzolan-based geopolymers increases their adsorption capacity for methylene blue dye stupendously while preserving the surface chemistry.

Keywords Pozzolan · Eco-adsorbents · Geopolymers · Adsorption · Methylene blue

1 Introduction

The problem of environmental pollution is still a topical issue because many industrial activities continue to generate various traditional and emerging pollutants, likely to create significant nuisance such as the destruction of aquatic fauna and flora [1]. Indeed, industrial effluents are among the major sources of environmental pollution. Additionally, these pollutants have the capacity to bioaccumulate along the food chain and accumulate in certain organs of the human body [2]. It is therefore essential to eliminate these toxic elements present in the industrial effluents or to reduce their concentrations below the admissible thresholds defined by the stipulated standards [1]. Faced by increasingly restrictive regulations, industries must obligatorily treat their effluents before discharging into the environment. To fight against this environmental issue, research in identification and elimination of water pollutants, such as methylene blue, directly involved in the appearance of imbalances in ecosystems like photosynthesis inhibition, under oxygenation, bioaccumulation or inducing serious disorders that can harm health such respiratory problems or even lead to death, both in animals and humans, is ever increasing [3].

✉ Sylvain Tome
sylvatome@yahoo.fr

✉ David Daniel Joh Dina
dinadavidcr@yahoo.com

[1] Department of Chemistry, Faculty of Science, University of Douala, P.O. Box 24157, Douala, Cameroon

[2] Department of Physical Sciences, Kaimosi Friends University College, P.O. Box 385-50309, Kaimosi, Kenya

[3] Institut für Anorganische Chemie und Strukturchemie, Universität Düsseldorf, Universitätsstr, 1D-40225 Düsseldorf, Germany

For this purpose, various classical pollutant removal techniques are used namely coagulation, flocculation, filtration, advanced oxidation processes (AOPs) and adsorption onto activated carbons. Though traditional approaches are insufficient in removing dyes from water to molecular levels, advanced oxidation processes are very expensive and toxic by-products are formed in the process of dye removal [4]. On the other hand, activated carbon is very expensive and the cost of regeneration is also very high [5]. The development of eco-friendly and cost-effective technologies are more and more desired to preserve the environment and for sustainability, respectively. Among the different treatment processes of dye-containing water effluents, adsorption stands out to be one the techniques relatively easy to use, easy to set up and of diverse variety of adsorbents that can used such as: biomass-derived activated carbons, clays and pozzolans among others [6]. The latter is an abundant and inexpensive natural resource in the world. Cameroon is counted among the largest producers of natural pozzolan, producing approximately 600 Kt/year [7]. It consists mainly of oxides of silicon, aluminum and iron (SiO_2, Al_2O_3 and Fe_2O_3) [8]. Pozzolan is used as a raw material in cement plants and in water treatment [9, 10]. However, its use in the field of adsorption is still limited due to its low adsorbing power, relative to other adsorbents [10]. For judicious use of this natural resource, its adsorption characteristics must be improved. Several works on the synthesis and adsorption of industrial contaminants onto geopolymers based on clays and fly ashes have been reported in literature [11–13]. These studies demonstrate the efficiency of geopolymers in the elimination of dyes from water effluent. However, the rarity of industrial waste precursors in many developing countries especially in remote areas, relative to pozzolan, limits their exploration. The transformation of the pozzolan into amorphous zeolite (geopolymer) is a sustainable and inexpensive way for its utilization as adsorbent for water treatment. However, geopolymerization only does not guarantee a high adsorbing product [14]. Consequently, several additives have been evaluated for amelioration of the adsorption characteristics of geopolymers. Singhal et al. [15] reported the use of Cetyl trimethylammonium bromide (CTAB) to improve the textural characteristics of metakaolin-based geopolymer. Other approaches include the chemical modification using bivalent metallic ions such as nickel, zinc and barium [16, 17]. These methods have their inherent limitations. CTAB is not only expensive but also changes the surface chemistry of the geopolymer. Alteration of the constitution of the geopolymer introduces site specific interactions that may induce specificity in the uptake of pollutants. Additionally, incorporation of bivalent heavy metals may cause secondary water pollution in case of leaching from the geopolymer framework. Simple, low-cost and environmentally benign methods are required for ameliorating the textural and adsorption characteristics of geopolymers. Hydrogen peroxide is known to decompose quickly in alkaline solution, the preparation conditions for geopolymer synthesis. The oxygen so-generated could be trapped in the geopolymer structure thus improving its porosity parameters and hence its adsorption performance while preserving its surface chemistry. Yuanyuan et al. [18] fabricated hydrogen peroxide modified metakaolin-based geopolymer for the removal of copper ions from water. Though the authors reported the surface area of the modified geopolymer (53.95 m^2/g), the study is silent on the textural characteristics of the unmodified geopolymer. Additionally, the adsorption capacity of the geopolymer (52.63 mg/g) was compared against a commercial spherical 4A molecular sieve (35.90 mg/g) and not a geopolymer prepared under similar conditions without hydrogen peroxide. The role of hydrogen peroxide in improving or diminishing the adsorption capacity of the geopolymer could neither be quantitatively accounted for nor inferred. Elsewhere, Liu et al. [19] prepared fly ash based geopolymer (GEO), hydrogen peroxide modified (GEOH), and hydrogen peroxide/oleic acid modified (GEOO) geopolymers. Though, GEOO had considerably high BET surface area (67.62 m^2/g), the surface areas of GEO and GEOH were not reported and therefore the individual contribution of hydrogen peroxide was unaccounted for. Furthermore, the adsorption performance for the removal of methylene blue was only examined for GEOO with a maximum adsorption capacity of 50.7 mg/g. As such, the role of hydrogen peroxide in both textural and adsorption characteristics of geopolymers is yet to be reported, and specifically for pozzolan-based geopolymers. The objective of this work was to ameliorate the adsorption characteristics of pozzolan-based geopolymers by preparation of a hydrogen peroxide modified pozzolan-based geopolymer as an eco-adsorbent. The effects of incorporation of hydrogen peroxide on the textural, structural and adsorptive performance for the removal of methylene blue dye from aqueous solution under various experimental conditions were examined and are herein reported.

2 Materials and Methods

2.1 Geopolymer Synthesis

The pozzolan used as a source of aluminosilicate was obtained from the locality of Mbouroukou in the Littoral region of Cameroon, crushed and sieved through 100 μm sieve to obtain uniform particle size. The alkaline activator solution was prepared by blending the sodium hydroxide (12 M from 98% purity sodium hydroxide flake) and commercial water glass (28.7 wt.% SiO_2, 8.9 wt.% Na_2O and 62.4 wt.% H_2O; density 1.37 g/mL). The ratio (liquid/liquid) of sodium hydroxide/commercial water glass was 2.4. The geopolymer was synthesized by mixing the alkaline solution and the pozzolan powder

in a liquid/solid ratio of 0.3. This blend was homogenized for 10 min using a mixer where a fresh paste was formed. To alter the porosity of the geopolymers, hydrogen peroxide in a mass ratio of 1% was added, as a blowing agent, to the paste previously left to rest for 30 min and it was then poured into cylindrical PVC moulds. Once moulded, the whole was mechanically compacted for one minute and then put in an oven (MEMMERT B2162385) at 60 °C for 24 h, then removed and left to rest for 4 days. The geopolymer samples obtained without (pristine) and with incorporation of hydrogen peroxide labeled GP_0 and GP_1, respectively, were then dipped in acetone for 2 h to stop the geopolymerization process, then dried in the oven at 60 °C for one hour. They were then crushed, sieved and washed until a neutral pH is obtained, then dried in an oven for 6 h.

2.2 Materials Characterization

The pozzolan and the synthesized geopolymers were subjected to various physico-chemical characterizations in order to determine chemical composition, textural properties, mineralogical composition, surface functional groups, thermal behavior, internal structure and morphology by the following methods:

2.2.1 X-Ray Fluorescence

The x-ray fluorescence spectrometry (XRF) method (Bruker-SRS 3400) was used to determine the bulk oxide composition of pozzolan.

2.2.2 Iodine and Methylene Blue Indices

The iodine and methylene blue indices are determined following the method used by Mbaye [20] to evaluate the microporosity and macroporosity of eco-adsorbents. The procedures are as follows:

Iodine Index In a 100 mL Erlenmeyer flask, 0.1 g of geopolymers previously dried in an oven at 110 °C for 24 h were brought into contact with 20 mL of 0.02 N iodine solution mixture stirred for 4 to 5 min and then filtered. Subsequently, 10 mL of the filtrate was titrated with sodium thiosulfate solution (0.1 N) using starch as the color indicator.

Methylene Blue Index In a 100 mL Erlenmeyer flask, 0.1 g of previously dried geopolymers and 50 mL of methylene blue solution were mixed, and the mixture stirred for 4 to 5 min and then filtered. The residual methylene blue concentration was determined using a UV - visible spectrophotometer (MERCK spectroquant Pharo 300 UV/visible instruments) at a wavelength of 662 nm.

2.2.3 The Point of Zero Charge (pH_{PZC})

The point of zero charge was determined following the protocol described by Karadag [21]. Briefly, six NaCl control solutions (0.1 M) with a pH between 2 and 12 are prepared. To 20 mL of each of these solutions is added 0.1 g of adsorbent. The suspensions obtained are left to stand for 8 h under stirring at room temperature, and their pH values are accurately determined using a pH meter (VOLTCRAFT PH-100ATC) after filtration.

2.2.4 Nitrogen Adsorption and Surface Area Measurement

Total surface area and micropore surface area of powder geopolymers were determined using N_2 adsorption at 77 K in a Quantachrome Autosorb AS6AG Station 3 instrument (Institute of Inorganic chemistry and structural of Dusseldorf, Germany). The values of the two properties were calculated from experimental isotherms using the Brunauer-Emmett-Teller (BET) analysis method.

2.2.5 X-Ray Diffraction

The crystalline phases present on the samples were determined using X-ray diffraction (XRD). An X-ray Powder Diffractometer (Bruker D8 Discovery, US) with the Bragg-Bretano theta-theta configuration, using a CuKα radiation at 27.5 kV and 25 mA was used for characterization. Spectra was obtained in the 2θ range from 6° to 80° with a step of 0.02° and 1 s per step scan rate.

2.2.6 Fourier Transform Infra-Red Spectroscopy (FTIR)

Fourier Transform Infra-Red spectroscopy (FTIR) permits the identification of functional groups on the surface of these materials. FTIR analysis of the samples was carried out by a FTIR Spectrophotometer (Nicolet 5700 FTIR, Thermo Electron Corporation) between 4000 and 400 cm^{-1} wavenumbers.

2.2.7 TGA/DTA Analysis

Thermogravimetric (TGA) and derivative thermogravimetric (DTG) curves of pozzolan (Pz) and geopolymers (GP_0 and GP_1) were obtained on a TA Instruments model NETZSCH TG 209F3 equipment with platinum sample crucibles. The powder was heated in Nitrogen (purge rate of 200 mL/min) at 6 °C/min.

2.2.8 Scanning Electron Microscopy

Microscope equipped with Energy Microstructure analysis was carried out in some selected specimens by HITACHI

S-3400 N Scanning Electron Dispersive X-ray Spectrometry analysis (EDS), operating at 15.0 kV.

2.3 Adsorption Experiments

Methylene Blue (MB) ($C_{16}H_{18}ClN_3S_xH_2O$) solutions were prepared at pre-defined concentrations for adsorption experiments.

The adsorption experiments were carried out in batches at different initial values of dye concentrations (10, 20, 30, 40 and 50 mg/L) and contact time using a precisely weighed quantity of adsorbents (0.1 g) into a 50 mL diluted solutions. After equilibration of 30 min for GP_1 material and 50 min for the GP_0 material, the absorbance of residual solutions was measured using a spectrophotometer (MERCK spectroquant Pharo 300 UV/visible instruments) at a wavelength of the MB (662 nm).

The adsorption capacity at a given time and the percent removals (%R) of methylene blue were calculated using the following equations:

$$qt = \frac{(C0-Ct)V}{m} \quad (1)$$

$$R(\%) = \frac{(C0-Ct) \times 100}{C0} \quad (2)$$

Where:

q The quantity adsorbed at time t (mg/g); C_0: The initial dye concentration (mg/L);

C_t The dye concentration at time t (mg/L); V: The volume of the solution (mL) and.

m The mass of the adsorbent in solution (g).

2.3.1 Effect of Contact Time

The tests were carried out by mixing in a reactor, in turn, 0.1 g of each geopolymer with 50 mL of the MB solution with a concentration of 50 mg/L. The homogenization of the mixtures is ensured by a magnetic stirrer at a stirring rate of 120 rpm during time intervals of 10, 20, 30, 40, 50 and 60 min.

2.3.2 Effect of the Initial Concentration

Diluted methylene blue solutions of 50 mL at different concentrations (10, 20, 30, 40 and 50 mg/L) were prepared and introduced into 5 reactors. A mass of 0.1 g of different geopolymers was added to each of these reactors and the mixture was stirred until the fixed equilibrium times of 30 min for GP_1 material and 50 min for the GP_0 material, respectively, filtered and residual MB determined.

2.3.3 Effect of pH

The effect of pH was examined by varying the pH of the MB solution from 2 to 12 using a solution of hydrochloric acid HCl (0.1 N) or caustic soda NaOH (0.1 N) depending on the desired pH.

2.3.4 Effect of Adsorbent Dosage

To various MB solutions with a concentration of 50 mg/L, masses of 0.05, 0.1, 0.2, 0.3, 0.4 and 0.5 g of each geopolymers, singly, was added and stirred at time intervals of 30 min for GP_1 material and 50 min for the GP_0 material. Subsequently, the different samples were filtered and residual MB concentration determined.

2.3.5 Effect of Temperature

A fixed mass (0.1 g) of different geopolymers was added to 50 mg L^{-1} of MB solutions (50 mL). The temperatures were adjusted between 309 and 339 K and the contents agitated until equilibration (30 min for GP_1 material and 50 min for the GP_0 material) and the residual dye concentration in solution determined.

3 Results and Discussion

3.1 Geopolymerization Mechanism

Figure 1 displays the different steps of the polycondensation reactions of activated pozzolan in a basic medium in the presence of hydrogen peroxide as a blowing agent. The mixture of the pozzolan with alkaline solution forms a geopolymer paste. The addition of hydrogen peroxide (H_2O_2) to this paste led to a prompt effervescence of the paste due to the release of dioxygen from the decomposition of H_2O_2. In this paste, the dissolution reactions of the active 'alumino-ferro-silicate' phases also occur. This dissolution generates oligomers which polymerize to form porous geopolymer phases. The water released by the decomposition of hydrogen peroxide combines with that of the activating solution to promote geopolymerization. However, the excess of water, at the end, is diffused to the surface, creating micro-cavities.

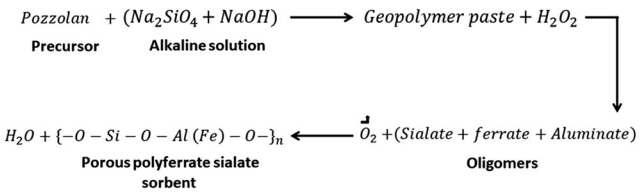

Fig. 1 Mechanism for hydrogen peroxide modified pozzolan-based geopolymer

Table 1 Chemical composition of pozzolan (Pz)

Oxides	SiO_2	Al_2O_3	CaO	Fe_2O_3	Na_2O	K_2O	MgO	Cl	SO_3	LOI
Pz (%)	47.74	15.36	8.25	12.88	3.62	1.11	6.45	–	–	0.66

3.2 XRF Analysis

The chemical composition of pozzolan, as determined by XRF analysis, is presented in Table 1. The main oxides in pozzolan are SiO_2, Al_2O_3 and Fe_2O_3 constituting 75.98%. Considering the potential reactivity of these oxides, the pozzolan was considered suitable for the development of geopolymers [22].

3.3 Textural Properties

3.3.1 Diameter, Pore Volume and Specific Area

Table 2 shows the results from the analysis of N_2 adsorption-desorption isotherm curves (Fig. 2) as well as the iodine and methylene blue indices. It can be seen that the addition of hydrogen peroxide, which decomposes into water molecules and oxygen during synthesis, appreciably increased the specific surface area, as well as the total pore volume within the material from 4.344 to 5.610 m^2/g and 6.022 to 9.747 ($\times 10^{-3}$ cm^3/g) for GP_0 and GP_1, respectively. The low values of iodine (444.150 m/g for GP_0 material and 571.050 m/g for GP_1 material) and methylene blue (20 m/g for GP_0 material and 23.680 m/g for GP_1 material) indices indicate that these geopolymers are very mesoporous. This is confirmed by the pore diameters (respectively 105.800 and 103.700 Å for GP_0 geopolymer and GP_1) which are between 2 and 50 nm) [23]. In addition, these both samples have displayed a characteristic type IV nitrogen adsorption–desorption isotherm in accordance with the IUPAC scheme of classification, as shown in Fig. 2 [24]. Hysteresis loop in the P/P_0 range of 0.4–0.9 denotes the presence of mesopores (pores in the range of 2–50 nm). The slight variation in the N_2 adsorption–desorption isotherms from standard type IV isotherm could be related to the existence of hetero-sized pores [25].

3.3.2 Point of Zero Charge pH_{PZC}

As for the pH at the point of zero charge (Fig. 3), it can be seen that the different geopolymers have the same pH_{PZC} (7.5). These values are comparable to those reported by Sarkar [16] for an alkali-activated Linz Donawitz (LD) slag. However, it also suggests that the incorporation of hydrogen peroxide during synthesis did not affect the surface functional groups. At solution pH values below the pH_{PZC}, these materials carry a net positive surface charge and a net negative surface charge at pH values higher than the pH_{PZC} [26].

3.4 Functional Groups Analysis by FTIR

The FTIR spectrum in Fig. 4 shows the vibration bands of the different materials recorded between 4000 and 400 cm^{-1}. The pozzolan presents the following vibration bands: the first one between 3550 and 3400 cm^{-1} corresponds to the elongation vibrations of the O-H bonds of water molecules [27]. The band around 1650 cm^{-1} is attributed to the deformation vibrations of the H-O-H bond of water molecules [28]. The bands centered between 1045 and 977 cm^{-1} corresponds to the symmetrical and asymmetrical elongations of the Si-O-Si and Si-O-Al bonds [29]. The bands between 913 and 736 cm^{-1} is related to the symmetrical vibrations of the Al-O and Al-OH. The bands around 550 and 460 cm^{-1} correspond to the symmetrical elongations of Si-O-Si, Al-O-Al, Si-O-Fe and deformations of the Si-O-Si, O-Si-O bonds, respectively. Comparing the spectrum of the precursor (Pz) with those of the geopolymers (GP_0 and GP_1), it is observed a shift of the main band of aluminosilicates from ~1023 to ~1036 cm^{-1}. This shift reflects a restructuring of the aluminosilicate phases present in the Pz material. It is also observed a decrease in intensity of the bands of aluminosilicates (1023 cm^{-1}),

Table 2 Physical properties of the different geopolymers

Adsorbents	Pores total volume ($\times 10^{-3}$ cm^3/g)	Pores diameter (Å)	specific surface (m^2/g)	Iodine number (m/g)	MB number (mg/g)	pH_{PZC}
GP_0	6.022	105.800	4.344	444.150	20.000	7.5
GP_1	9.747	103.700	5.610	571,050	23.680	7.5

silicates (760 cm^{-1}) and ferrates (436 cm^{-1}). This phenomenon confirms the dissolution of these phases in alkaline medium [30].

3.5 X-Ray Diffraction Analysis (XRD)

The diffractograms of the two studied geopolymers GP_0 and GP_1 and aluminosilicate source (Pz) used for their synthesis are shown in Fig. 5. The precursor is made in anorthite (An), $Na(AlSi_3O_8)$ (PDF#01–073-6461), feldspar-Na(F), $(NaAlSi_3O_8)$ (PDF#01–083-6911), forsterite (Fs), (Mg_2SiO_4) (PDF # 85–1462), diopside sodian (Ds), Ca(Mg, Fe, Al)(Si, Al)$_2O_6$ (PDF#38–466), diopside alumina (Da), Ca(Mg, Fe, Al) (Si, Al)$_2O_6$ (PDF#38–0466), augite(A) $(Ca_{0.61}Mg_{0.76}Fe_{0.49}(SiO_3)_2$, (PDF #76–0544) and hematite(H), Fe_2O_3 (PDF#03–0812) as mineral phases. Comparing the diffractograms of the aluminosilicate source (Pz) to that of eco-adsorbent whitout blowing agent (GP_0), it is observed that all the original peaks are present conforming the low dissolution mentioned at the FTIR section. There is no noticeable shift of the amorphous hump located between 20° and 35° indicating the low transformation of the aluminosilicate phases to geopolymer networks. Observing also the diffractograms of the eco-adsorbents obtained without and whit addition of hydrogen peroxide (GP_0 and GP_1), it is noticed the disappearances of the peaks at 32°, 36° and 63°. This fact reveals a probable dissolution of diopside alumina and diopside sodian minerals in hydrogen peroxide medium.

3.6 TGA/DTA Analysis

Figure 6 shows the thermograms of the precursor (Pz) (Fig. 6a) and the geopolymers (GP_0 (Fig. 6b) and GP_1 (Fig. 6c)). These thermograms show that the respective mass losses of 1.2% for Pz and 0.7% for GP_0 and GP_1 recorded between 27 and 400 °C reflect endothermic reactions. This is linked to the losses of structural and external molecules of water adsorbed by these materials. Comparing the thermograms of Pz (Fig. 6a) and GP_0 (Fig. 6b), an endothermic peak centered at 205 °C for GP_0 is observed. This shows that GP_0 contains more structural water than the precursor [31], which is evident because the activation of the aluminosilicate precursor (Pz) leads to a hydrated condensed phase namely sodium aluminate silicate hydrate (N-A-S-H). Comparing the thermograms of the eco-adsorbents GP_0 (Fig. 6b) and GP_1 (Fig. 6c), it is observed the mass loss of GP_1 (0.3%) is twice that of GP_0 (0.15%) in zone (1), thus revealing the presence of a considerable amount of water in the structure of GP_1 resulting from the decomposition of hydrogen peroxide. On the other hand, in zone (2), the mass loss of about 0.4% attributable to the endothermic dihydroxylation reaction (around 200 °C) for GP_1 is slightly lower than that for GP_0 (0.55%) probably due to a low thermal conductivity as

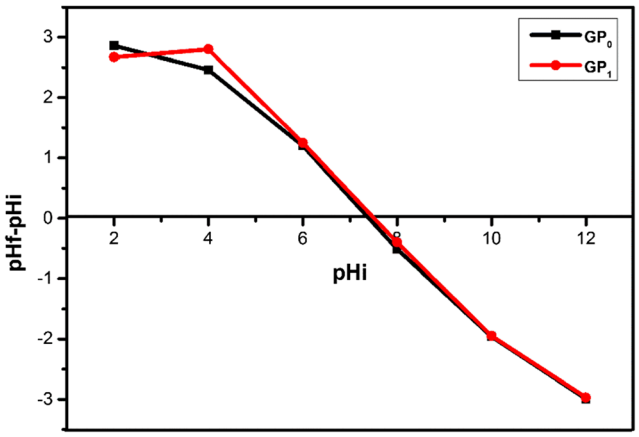

Fig. 3 Point of Zero Charge of geopolymer materials

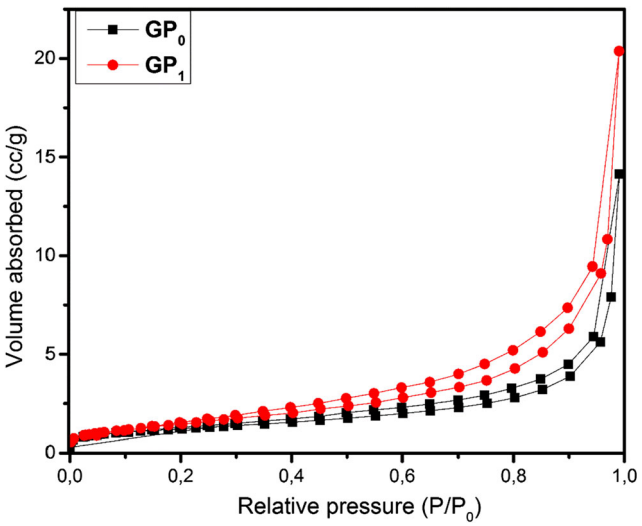

Fig. 2 N_2 adsorption-desorption isotherms of eco-adsorbents materials

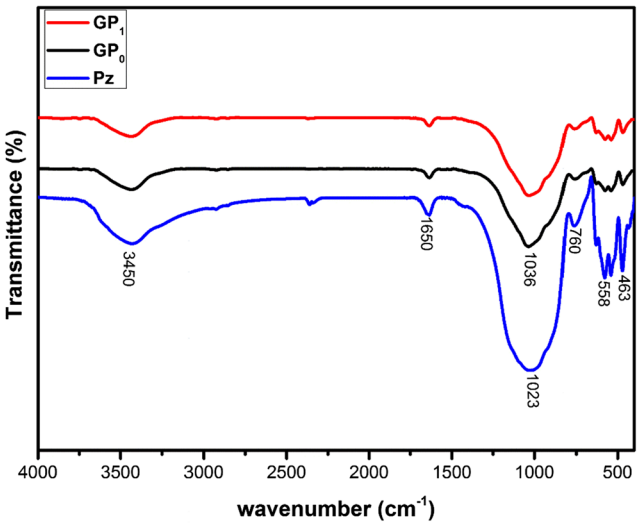

Fig. 4 FTIR of the samples Pz, GP_0 and GP_1

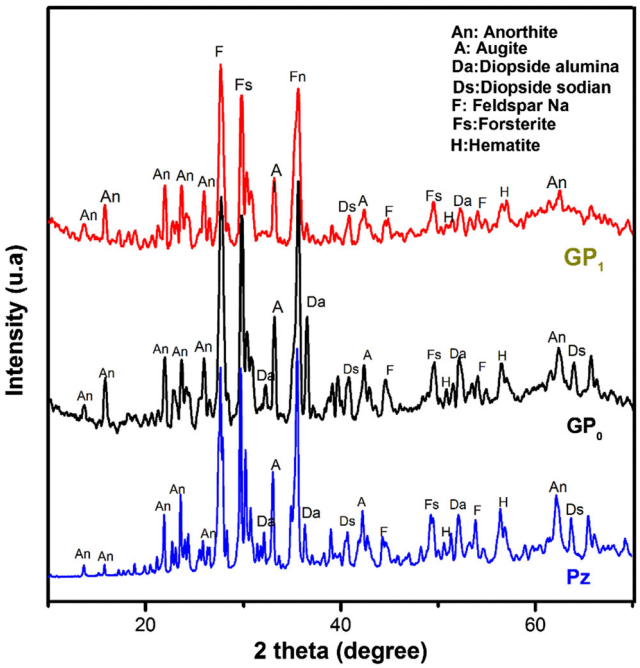

Fig. 5 XRD patterns of precursor and GP_0 and GP_1 geopolymer

the temperature becomes higher in this material reflecting the presence of a higher pore volume as reported by Kamseu et al. [32]. The lack of organic compound loss up to 600 °C is consistent with the LOI results (Table 1) which showed that pozzolan contains a small amount of organic matter.

3.7 Scanning Electron Microscopy and Energy Dispersive X-Ray Analysis (SEM/EDX)

Figure 7 shows the micrographs of the Pz, GP_0 and GP_1 materials associated with their elemental compositions (Table 3). The Fig. 6a shows that the pozzolan is mainly made of crystalline phases and the EDX analysis reveals that these phases are aluminosilicate minerals, corresponding to those mentioned in the XRD section. Comparing the microstructural of Pz to that of GP_0 material (Fig. 6b), the observed densification of the microstructure of GP_0 material is due to polymerization/polycondensation of aluminosilicate phases to geopolymer networks. The micrograph (Fig. 6c) presents the capillary pores dispersed on the microstructure of geopolymer network. This fact discloses that the

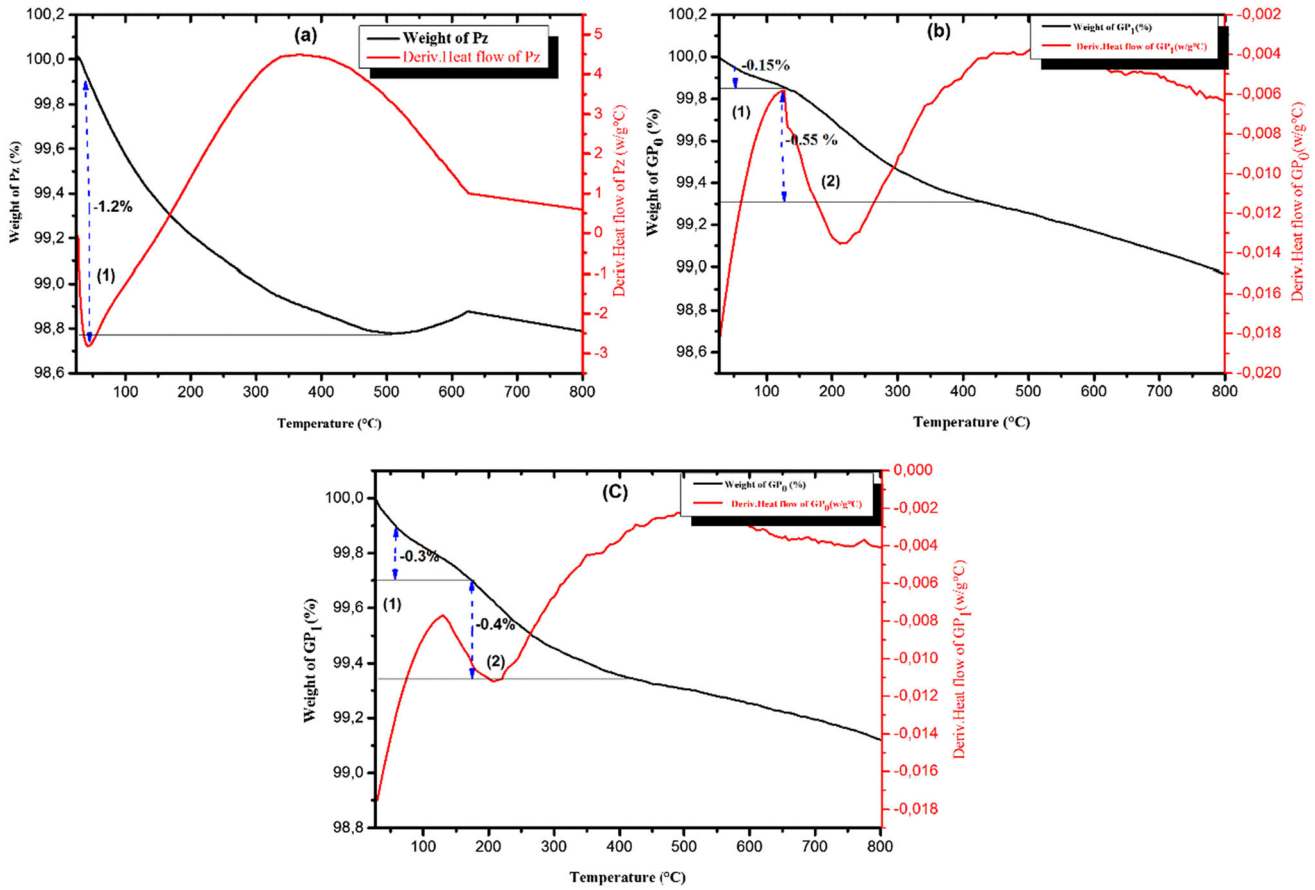

Fig. 6 Thermal behavior of pozzolan (**a**) and geopolymers (GP_0 (**b**) and GP_1(**c**))

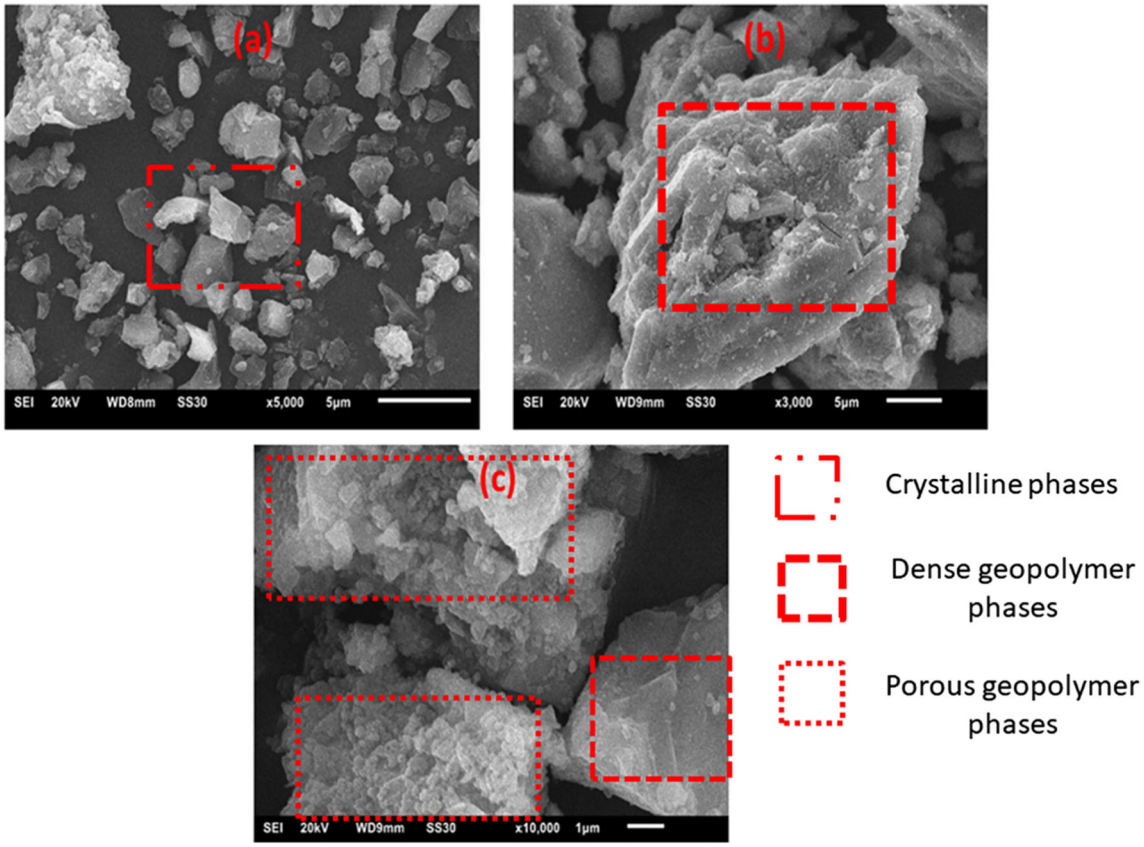

Fig. 7 Scanning electron Microscopy of Pz (a), GP_0 (b) and GP_1 (c)

blowing agent affect the structure and the microstructure of geosorbent. The elemental composition of both materials confirms that silicate, aluminate and ferrate phases participate to the geopolymerization and the negative charges of geopolymer networks are balanced by Na^+, K^+, Ca^{2+} and Mg^{2+} ions. Moreover, considering the values of Si/Fe ratios more significant than those of Si/Al (Table 3), it can be concluded that GP_0 and GP_1 geoadsorbents are made of poly (ferro- sialate-siloxo) chains. It should also be noted that the presence of cracks and capillary pores on the surface of the geopolymers GP_0 (Fig. 6b) and GP_1 (Fig. 6c) will constitute the access routes of the adsorbates to active sites of the framework during the adsorption process.

3.8 Influence of pH

Figure 8 represents the influence of pH on the adsorption capacities of MB generally revealed that the fixation of MB is unfavorable in acidic medium on the two eco-adsorbents due the electrostatic repulsion between the MB molecules and positively charged surfaces of these materials. In addition to this repulsion at pH below 5, an increased competition between MB cations and hydrogen ions (H^+) for the active sites

Table 3 EDX analysis of the Pz, GP_0 and GP_1 materials

Element	Si	Al	Fe	Ca	Mg	Na	K	O	Si/Al	Si/Fe
Material	**Pz (a)**									
%Element	15.11	5.80	3.12	2.39	1.63	1.46	0.38	43.71	2.60	4.84
Material	**GP_0 (b)**									
%Element	15.91	6.98	5.58	6.47	2.93	2.82	0.52	45.17	2.27	2.85
Material	**GP_1 (c)**									
%Element	8.77	4.26	2.77	2.68	1.86	1.66	0.25	26.18	2.06	3.16

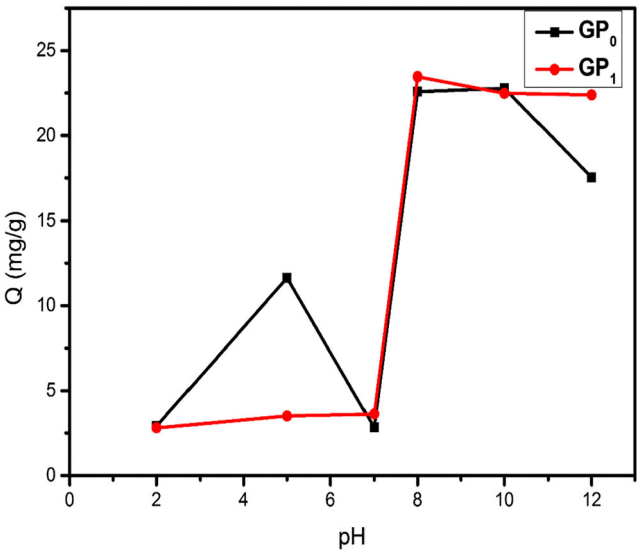

Fig. 8 Influence of pH on the adsorption capacity of the different geopolymers

of the GP_0 compared to GP_1 is implied. In contrast, in a basic medium (at pH above 7.5), the GP_0 and GP_1 surfaces became more negative and the uptake of MB cations increased due to electrostatic attractions. The increase in negatively charged adsorption sites is attributed to deprotonation of the silanols (SiO-H) or aluminol (AlO-H) groups. This is consistent with the reports by Marouane and co-workers reported for MB sequestration by a metakaolin-based geopolymer [13].

3.9 Effect of Adsorbent Dose

Figure 9 shows that a mass of 0.2 g of geopolymers (GP_0 and GP_1) is capable to sequester at most 97.79% and 99.39% of the initial MB in solution, respectively. Beyond this mass, the quantities of MB adsorbed decrease and with no appreciable change, indicating an agglomeration of certain adsorption sites due to excess mass [33]. It will, therefore, be useful to

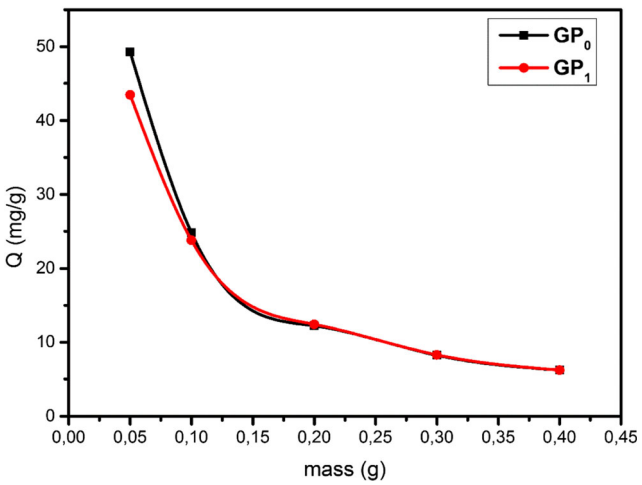

Fig. 9 Influence of Adsorbent Dose

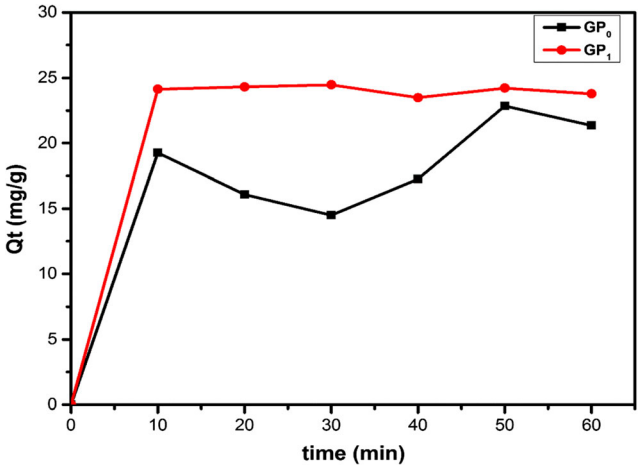

Fig. 10 Effect of the MB contact time on the adsorption capacities of the different geopolymers

work with adsorbent doses less than or equal to 0.2 g to avoid inefficient overdosing.

3.10 Contact Time

Figure 10 represents the influence of contact time on the MB uptake by the GP_0 and GP_1. At the very beginning of the adsorption process, a rapid increase of the adsorbed quantities is observed. This process stabilizes after 10 min with the appearance of an equilibrium stage for both materials. Beyond 10 min a desorption phenomenon is observed which extends from the 10th to the 20th minute for the geopolymer GP_1 and from the 10th to the 30th minute for the geopolymer GP_0 where this phenomenon is very pronounced. The adsorption process is considered to have reached the pseudo-equilibrium state after 50 min for the GP_0 material and 30 min for the GP_1 material with adsorbed quantities of MB of 22.860 mg/g and 24.470 mg/g, respectively. This kinetics can be explained by the fact that at the beginning of the process, there is a rapid occupation of the vacant adsorption sites by the MB molecules. As for the desorption phenomenon, it is due to the size of MB molecules (14.47 Å) [34] which is much smaller than the pore diameters of the GP_0 and GP_1 and allows detachment of weakly adsorbed molecules.

3.11 Kinetic Study

In order to minimize errors due to linear regression as discussed in the works of Shikuku al. [35], and Chuncai al. [36], the non-linear regression method for the pseudo-first order, pseudo-second order and vermeulen kinetic models was applied to the experimental data to determine the best-fitting model, adsorption rate and predict the mechanism

controlling the adsorption kinetics of methylene blue onto the geopolymers.

3.11.1 Pseudo-First-Order Model or Lagergren Model (PFO)

The general Lagergren (1898) first-order rate expression is expressed as follows:

$$\frac{dq_t}{dt} = k_1(q_e - q_t) \tag{3}$$

Where q_t (mg/g) is the adsorbed amount at time t (min), k_1 (min^{-1}) is the pseudo-first-order rate constant and q_e is the equilibrium value of q. Integration of Eq. (4) with the initial condition q = 0 at t = 0 gives

$$q = q_e\left(1 - e^{-k_1 t}\right) \tag{4}$$

The initial value for k_1 may be obtained by using the half adsorption time $t_{1/2}$ (defined as the time when $q_t = q_e/2$) estimated from the kinetic data and the following relationship for the PFO.

Model.

$$K_1 = \frac{\ln 2}{t_{1/2}} \tag{5}$$

$$S_{rate} = K_1 q_e \tag{6}$$

Where S_{rate} ($mg.g^{-1}.min^{-1}$) is the initial adsorption rate.

3.11.2 Pseudo-Second-Order (PSO)

McKay and Ho (1998) presented a model to characterize the kinetics of adsorption taking into account both cases of a rapid fixation of solutes at the most reactive sites and that of a slow fixation at the weak sites energies. The rate law is written as follows:

$$\frac{dq_t}{dt} = K_2(q_e - q_t)^2 \tag{7}$$

The integrated form can be written as.

$$q = \frac{K_2 q_e^2 t}{1 + K_2 q_e t} \tag{8}$$

An initial trial value for $k_2 q_e$ may be obtained by using the following relationship for the PSO model

$$K_2 q_e = \frac{1}{t_{1/2}} \text{ With } S_{rate} = k_2 q_e^2 \tag{9}$$

Where: K_2 ($g.mg^{-1}.min^{-1}$) is the pseudo-second-order rate constant and S_{rate} ($mg.g^{-1}.min^{-1}$) is the initial adsorption rate.

3.11.3 Vermeulen Model

The Vermeulen model is based on the assumption that intraparticle diffusion is the controlling mechanism of adsorption. It is also known as the Urano model or the Dumwald–Wagner model [37]. The integrated Vermeulen model can be expressed as

$$q = q_e\left(1 - e^{-Bt}\right) \tag{10}$$

An initial trial value for intraparticle diffusion constant B (min^{-1}) may be obtained by using the relationship for the Vermeulen model

$$B = \frac{\ln\left({}^{4}/_{3}\right)}{t_{1/2}} \tag{11}$$

Table 4 presents the parameters of the pseudo first-order, pseudo second order and intra-particle diffusion kinetic models. The pseudo-second order kinetic model (Fig. 11) is the best to describe the MB adsorption mechanism on geopolymers GP_0 and GP_1 compared to the other kinetics models studied with the coefficients of determination (R^2) values are closest to unity and the model-predicted quantities of MB adsorbed (19.521 mg/g and 24.073 mg/g, respectively) are very close to those obtained experimentally (22.858 mg/g and 24.473 mg/g, respectively). The adsorption mechanism is thought to take place in the following sequence: diffusion of the solute molecule towards the surface of the geopolymers, followed by displacement of the solute towards the

Table 4 Parameters obtained from kinetic models

Models	Parameters	GP_0	GP_1
Pseudo first order	K_1 (min^{-1})	1.996	2.523
	q_e (cal) (mg g^{-1})	18.550	24.069
	q_e (exp) (mg g^{-1})	22.858	24.473
	$t_{1/2}$ (min)	0.347	0.275
	Srate ($mg.g^{-1}.min^{-1}$)	37.030	60.726
	R^2	0.852	0.998
Pseudo second order	K_2 (g mg^{-1} min^{-1})	0.039	9.999
	q_e (cal) (mg g^{-1})	**19.521**	**24.073**
	q_e (exp) (mg g^{-1})	**22.858**	**24.473**
	$t_{1/2}$ (min)	1.316	0.004
	Srate ($mg.g^{-1}.min^{-1}$)	**14.837**	**5794.644**
	R^2	**0.858**	**0.998**
Vermeulen	B (min^{-1})	3.216	3.216
	q_e (cal) (mg g^{-1})	18.551	24.069
	q_e (exp) (mg g^{-1})	22.858	24.473
	$t_{1/2}$ (min)	0.0894	0.089
	R^2	0.852	0.998

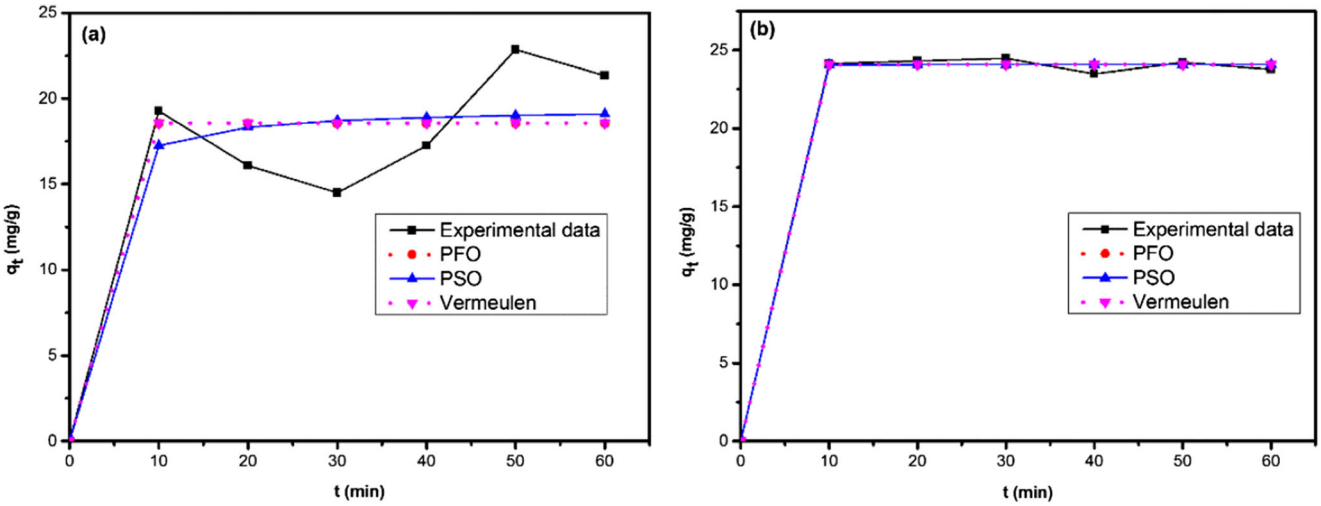

Fig. 11 PFO, PSO and Vermeulen models applied to the experimental kinetic data for the adsorption of MB on different geopolymers ((a) GP_0 and (b) GP_1)

interior of the pores and finally fixation of the solute towards the active sites inside the pores [38]. It also reflects the existence of interactions between the surface of the adsorbent and the adsorbate, suggesting a multi-mechanistic chemisorption mechanism [39]. Noteworthy, the initial adsorption rate for MB uptake by GP_1 was higher than GP_0. The fast adsorption of MB GP_1 is attributed to the larger surface area of GP_1 than GP_0 resulting to easier and faster access to the binding sites in GP_1. This reveals that the use of hydrogen peroxide as a blowing porogen during the synthesis modifies the textural properties (porosity and the specific surface area) but does not increase the identity of the binding sites as shown by the FTIR results.

3.12 Influence of Initial Concentration

From Fig. 12, the quantities adsorbed in MB increase linearly with the initial MB concentrations of 4.71–21.35 mg/g and 4.89–23.78 mg/g for GP_0 and GP_1 materials, respectively. This observation implies that an increase in MB concentration increases the diffusion and fixation of the solute molecules within the pores of these geopolymers.

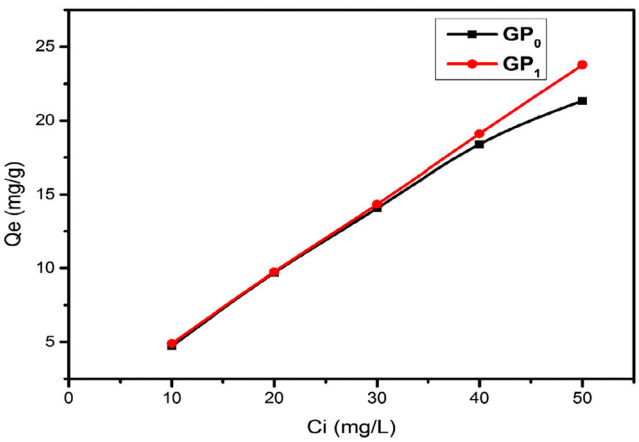

Fig. 12. effect of initial concentration

3.13 Isotherms Adsorption

Experimental equilibrium data were analyzed using five theoretical non-linear adsorption isotherms (Langmuir, Freundlich, Temkin, Dubinin-Radushkevich-Kaganer and Sips) to determine the model that best predicts the adsorption data and therefore best describes the adsorption mechanism of methylene blue on these eco-adsorbents.

3.13.1 Langmuir Isotherm

Langmuir isotherm (Langmuir, 1916) suggests a one–one association between adsorbate and adsorbent resulting in the formation of a monolayer. The adsorption data are validated by determining the uptake capacity (q_e) and adsorption parameters using Eq. (12) where q_e (mg/g) is the amount adsorbed at equilibrium and C_e (mg/L) is the equilibrium concentration.

$$q_e = \frac{Q_m K_L C_e}{1 + K_L C_e} \tag{12}$$

Where q_e is the amount of MB adsorbed at equilibrium (mg g^{-1}), C_e is the MB concentration in the aqueous phase at equilibrium (mg L^{-1}), Q_m is the Langmuir maximum adsorption capacity (mg g^{-1}) and K_L is the Langmuir constant (L g^{-1}). The dimensionless separation factor, R_L, was calculated using Eq. (13) [40]. The R_L value indicates whether the adsorption is favorable ($0 < RL < 1$), unfavorable ($R_L > 1$), linear ($R_L = 1$), or irreversible ($R_L = 0$) [38].

$$R_L = \frac{1}{1 + K_L C_0} \tag{13}$$

3.13.2 Freundlich Isotherm

The Freundlich isotherm model (Freundlich, 1906) is an empirical equation that is applied to multilayer adsorption. This model assumes that the surface of the adsorbent is heterogeneous and active sites and their energies distribute exponentially. The Freundlich isotherm is expressed as Eq. (14):

$$q_e = K_F C_e^{1/n} \tag{14}$$

Where K_F is the Freundlich constant (L g^{-1}) and the parameter n is a dimensionless constant.

3.13.3 Dubinin-Radushkevich Kaganer Isotherm

The Dubinin-Radushkevich-Kaganer (D-R-K) isotherm (Eq. 15) is applied to the adsorption process onto a microporous adsorbent. It estimates the energy of adsorption and distinguishes between physisorption or chemisorption nature of adsorption onto homogeneous and heterogeneous surfaces [40].

$$Q_e = Q_m \exp\left(-\beta \xi^2\right) \tag{15}$$

Where Q_e is the amount of adsorbate adsorbed per unit dosage of the adsorbent at equilibrium (mol/g) and Q_m is the theoretica monolayer saturation capacity (mol/g) [41]. The Polanyi potential (ε) is expressed as

$$\xi = RT \ln\left(1 + \frac{1}{c_e}\right) \tag{16}$$

The mean sorption energy E_a (kJ/mol) of the adsorbate (Eq.17) identifies the physical and chemical interactions between the adsorbate and adsorbent during the adsorption process.

$$E_a = \frac{1}{\sqrt{2\beta}} \tag{17}$$

3.13.4 Temkin Isotherm

The Temkin isotherm model contains a factor that explicitly takes into account the adsorbent–adsorbate interactions. The heat of adsorption of all the molecules in the layer would decrease linearly with coverage due to adsorbent–adsorbate interactions. The adsorption is characterized by a uniform distribution of binding energies, up to some maximum binding energy. The Temkin adsorption isotherm expression is shown in Eq. (18) [42].

$$q_e = B_T \ln(A_T C_e) \tag{18}$$

Where $B_T = RT/b_T$, b (J/mol) is the Temkin constant relating to the heat of sorption; A (L/g) is the Temkin isotherm constant. R is the universal gas constant (8.314 J/mol.K), and T (K) the absolute temperature.

Table 5 Parameters obtained from adsorption isotherms

Isotherms	Parameter	GP_0	GP_1
Langmuir	Q_{max} (mg/g)	23.897	30.102
	K_L (L/mg)	0.915	0.838
	R_L	0.021	0.023
	R^2	0.917	0.981
Freundlich	K_F (mg/g) $(L/mg)^{-1}$	10.183	13.242
	1/n	0.403	0.627
	R^2	0.884	**0.982**
D – R – K	Q_{max} (mg/g)	20.181	22.076
	E_a (KJ/mol)	1.036	1.374
	R^2	0.907	0.873
Temkin	A (L/g)	5.692	8.215
	ΔQ (KJ/mol)	5.953	7.152
	R^2	0.933	0.936
Sips	Q_{max} (mg/g)	24.440	366.196
	a_S	0.730	0.038
	B_S	1.1489	0.652
	R^2	**0.941**	0.981

3.13.5 Sips Isotherm

By identifying the problem of continuing increase in the adsorbed amount with an increase in concentration in the Freundlich equation, Sips proposed an equation that combines

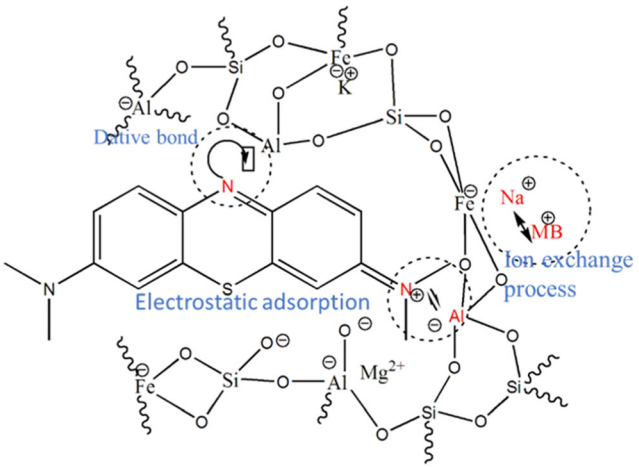

Fig. 13 Interaction mechanisms in the GP1-MB system

Table 6 Thermodynamic functions for MB uptake by GP_0 and GP_1

Adsorbent	Temp. (K)	ΔG (kJ mol^{-1})	ΔH (kJ mol^{-1})	ΔS (kJ mol^{-1})
GP_0	309	−16.02		
	319	−16.66		
	329	−17.92	32.20	0.15
	339	−20.84		
GP_1	309	−17.49		
	319	−18.91		
	329	−19.81	20.62	
	339	−21.31		0.12

the Freundlich and Langmuir isotherms. This produces an expression that exhibits a finite limit at sufficiently high concentration. This model is valid for predicting the heterogeneous adsorption systems and localized adsorption without adsorbate-adsorbate interactions. The Sips isotherm model is given by Eq. (19):

$$Q_e = \frac{Q_{ms} a_s C_e^{B_s}}{1 + a_s C_e^{B_s}} \tag{19}$$

Where Q_{ms}, a_s and B_s are the isotherm constants. The constant B_s is the heterogeneity index.

The assessment of the validity of the results in Table 5 was based on the values of the coefficient of determination, R^2. The equilibrium data was described by the models in the order Sips >Temkin >Langmuir > D-K-R > Freundlich model for the GP_0 and Freundlich > Sips >Langmuir > Temkin > D-K-R model for the material GP_1.

The Freundlich isotherm is appropriate to describe the adsorption mechanism of MB on the geopolymer GP_1 and the value of the Freundlich parameter *n* lower than 1, implies that the adsorption sites of this geopolymer are heterogeneous, consequently the adsorption is carried out in multilayer and the isotherm is linear of H type (Fig. 14b) [43].

The Sips isotherm, was the most appropriate to describe the adsorption of MB on geopolymer GP_0 (Fig. 14a). The heterogeneity factor (Bs) of 1.14893 greater than unity, indicates heterogeneity of the system resulting from the interaction adsorbent-adsorbate [44]. The adsorption capacities can be estimated using the sips isotherm model, therefore it follows that the adsorption capacity of MB are high on the GP_1 (366.196 mg/g) that GP_0 (24.440 mg/g). This could be justified simply by the high pore volume and specific surface area that GP_1 has compared to GP_0 (Table 2). The high adsorption capacity of MB GP_1 material (15 times higher than that of GP_0 material) is also justified by the various phenomena possibly taking place within the multiple pores (Fig. 13) such as:

- Electrostatic interactions between the negative sites of geopolymers and positives sites of MB.
- Ions exchange between the MB cations and counter ions (Na^+, K^+, $Ca^{2+}$and Mg^{2+}).
- Formation of dative bonds between the nitrogen doublets of MB molecules and the empty quantum cells of the GP_1 material.

The D-R -K model shows that the adsorption energy of the two synthetic materials are less than 8 kJ/mol, which suggests

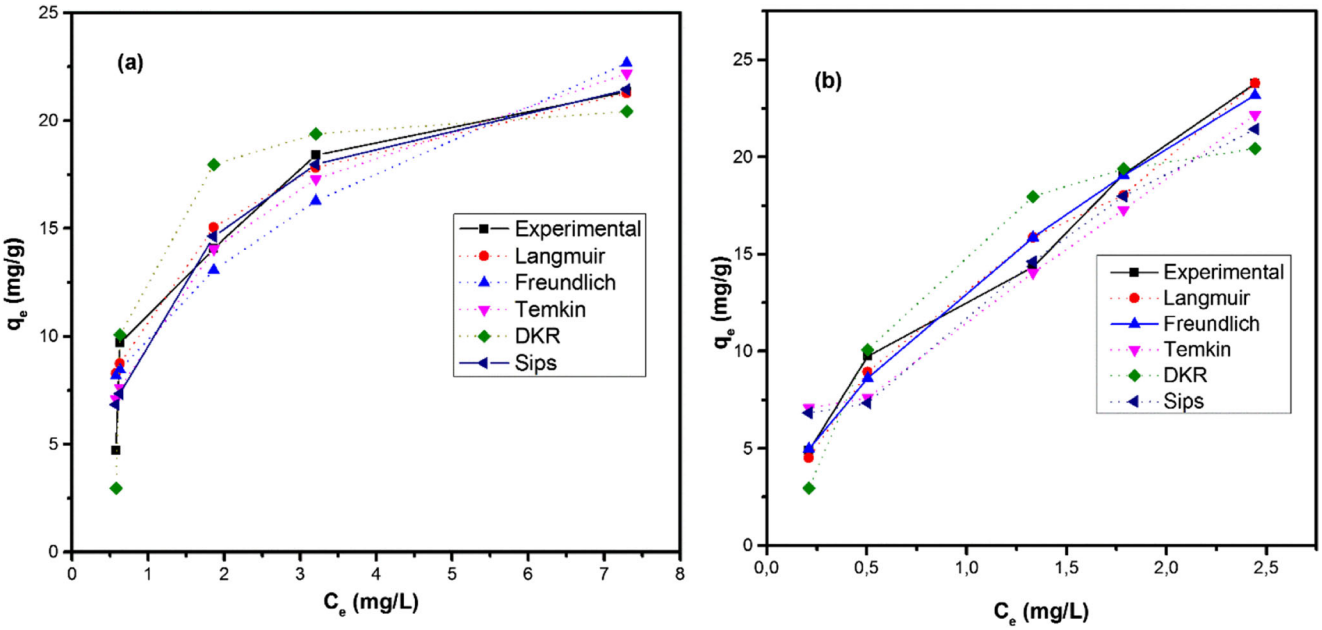

Fig. 14 Adsorption isotherm plots for MB onto (**a**) GP_0 and (**b**) GP_1 materials

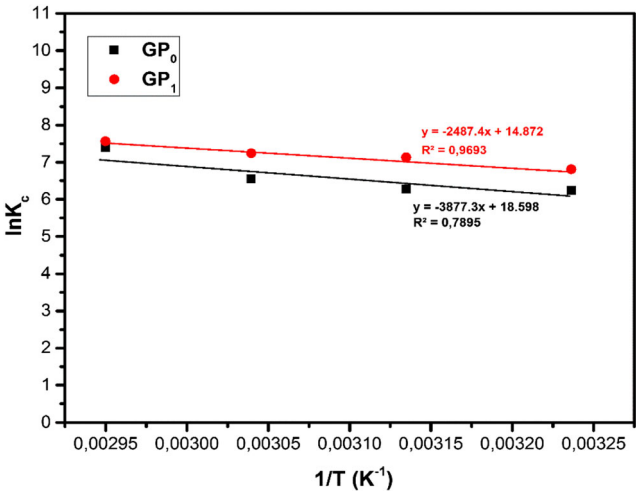

Fig. 15 Isotherm plot of van't Hoff

that physisorption is the dominant adsorption mechanism [45].

3.14 Adsorption Thermodynamics

The effects of temperature and adsorption thermodynamics functions were evaluated in the temperature range 309–339 K. The thermodynamic functions, enthalpy change (ΔH), Gibb's free energy (ΔG), and entropy (ΔS) were calculated using Eqs. 20–23 and the calculated parameters for MB uptake are listed in Table 6.

$$\Delta G = -RT\ln K_c \tag{20}$$

$$K_d = \frac{C_{ads}}{C_e} \tag{21}$$

$$K_c = 1000K_d \tag{22}$$

$$\ln K_c = \frac{\Delta S}{R} - \frac{\Delta H}{R}\frac{1}{T} \tag{23}$$

Where K_c is the equilibrium constant (dimensionless), C_e is the residual dye concentration in the aqueous phase at equilibrium (mg L^{-1}) and C_{ads} is the dye concentration in the adsorbent at equilibrium (mg g^{-1}), K_d is the distribution coefficient (L/g) and the density of water is 1000 g/L. R is the gas constant (8.314 J mol^{-1} K^{-1}) and T is the temperature (K).

The positive enthalpy (ΔH) values confirm that adsorption of the MB on the eco-adsorbents is an endothermic reaction. The negative ΔG values, reveal the feasibility and spontaneity of MB removal on both geopolymers. The decrease in the magnitude of ΔG with rise in temperature implies the reaction becomes more and more spontaneous and the amount adsorbed increases with increased temperature consistent with an endothermic process (Fig. 15). The relatively low ΔG values correspond to a physical process. The positive values of entropy denote that the approach and distribution of MB molecules through the pores of GP_0 and GP_1 materials is disordered. In addition, the ΔH values below 40 kJ mol^{-1} indicate that the sorption of MB on these eco-adsorbents entails a physisorption mechanism, consistent with the prediction from D-K-R model [46].

4 Conclusion

The development the pozzolan-based eco-adsorbents was done by geopolymerization using hydrogen peroxide as a blowing agent with mass ratios 0 and 1%, labeled GP_0 and GP_1 respectively, in order to modify the textural properties and to evaluate their performance in removing the basic dye methylene blue in aqueous solution. The physico-chemical characteristics revealed that the incorporation of 1% blowing agent increased the specific surface are from 4.344 to 5.610 m^2/g. The increase in surface area resulted to an increase in adsorption capacity by 15 orders of magnitude from 24.4 to 366.2 mg/g for GP_0 and GP_1, respectively. The adsorption rates of methylene blue on the two eco-adsorbents were best described by the pseudo-second order kinetic model. The adsorption equilibrium data were best described by the Sips and Freundlich isotherms models for GP_0 and GP_1, respectively. Thermodynamically, it was determined that the adsorption of methylene blue onto eco-adsorbents is a physical and endothermic process. The results show that incorporation of hydrogen peroxide into pozzolan-based geopolymers increases their adsorption capacity for methylene blue dye stupendously relative under the experimental conditions reported. The products in addition to its use in the field of civil engineering as thermal insulation, they can also be used as adsorbent for the effective depollution of industrial effluents.

Supplementary Information The online version contains supplementary material available at https://doi.org/10.1007/s12633-021-01264-4

Acknowledgements We thank Institute of Inorganic chemistry and structural in Dusseldorf (Germany) for the characterization of raw materials and geopolymers samples.

Code Availability Not applicable.

Author Contributions David Dina, Sylvain Tome: Validation, Methodology, Writing - review & editing,

Visualization, original draft. Dzoujo T. Hermann, Jean T. Tchuigwa: Conceptualization, Methodology, Investigation, writing - original draft, resources. Victor O. Shikuku: Validation, Writing - review & editing. Alex Spieß: Validation, Writing - review & editing, Marie-Annie Etoh: Writing - review & editing, Visualization. David Dina, Marie-Annie Etoh, Christoph Janiak: Resources, Supervision.

Data Availability All data generated or analyzed during this study are included in this article.

Declarations

Consent to Participate Not applicable.

Consent for Publication Not applicable.

Conflict of Interest The authors declare that they have no conflict of interest.

References

1. Fatima Zohra Choumane, (2015) Elimination des métaux lourds et pesticides en solution aqueuse par des matrices argileuses, Thèse de Doctorat, Chimie de l'environnement
2. Brown MA, De Vito SC (2009) Predicting azo dye toxicity predicting azo dye toxicity. Crit Rev Environ Sci Technol (June 2013):37–41. https://doi.org/10.1080/10643389309388453
3. Dipa G, Bhattacharyya KG (2002) Adsorption of methylene blue on kaolinite. Appl Clay Sci 20:295–300
4. Alvares ABC, Dlaper C, Parsons SA (2013) Partial oxidation by ozone to remove recalcitrance from wastewaters – a review. Environ Technol 22:409–427
5. Badawi MA, Negm NA, Abou Kana MTH, Hefni HH, Abdel Moneem MM (2017) Adsorption of aluminum and Lead from wastewater by chitosan-tannic acid modified biopolymers: isotherms, kinetics, thermodynamics and process mechanism. Int J Biol Macromol 99:465–476. https://doi.org/10.1016/j.ijbiomac.2017.03.003
6. Sharma P, Kaur H, Sharma M, Sahore V (2011) A review on applicability of naturally available adsorbents for the removal of hazardous dyes from aqueous waste 151–195 183:151–195. https://doi.org/10.1007/s10661-011-1914-0
7. US Department of the interior and US Geological Survey (2010) Minerals yearbook, metals and minerals, vol 1. Government Printing Office, Washington DC
8. Billong N, Melo UC, Njopwouo N, Louvet F, Bonnet JP (2013) Physicochemical characteristics of Some Cameroonian pozzolans for use in sustainable cement like materials. Mater Sci Appl 4:14–21
9. Wamba AGN, Lima EC, Ndi SK, Thue PS, Kayem JG, Rodembusch FS, dos Reis GS, de Alencar WS (2017) Synthesis of grafted natural pozzolan with 3 aminopropyltriethoxysilane: preparation, characterization, and application for removal of brilliant green 1 and reactive black 5 from aqueous solutions. Environ Sci Pollut Res 24(27):21807–21820. https://doi.org/10.1007/s11356-017-9825-4
10. Kofa GP, NdiKoungou S, Kayem GJ, Kamga R (2015) Adsorption of arsenic by natural Pozzolan in a fixed bed: determination of operating conditions and modeling. Journal of Water Process Engineering 6:166–173. https://doi.org/10.1016/j.jwpe.2015.04.006
11. Fumba G, Essomba JS, Tagne GM, Nsami JN, Bélibi PDB, Mbadcam JK (2014) Equilibrium and kinetic adsorption studies of methyl Orange from aqueous solutions using kaolinite, Metakaolinite and activated Geopolymer as low cost adsorbents. Journal of Academia and Industrial Research (JAIR) 3:156–163
12. Novais RM, Ascensão G, Tobaldi DM, Seabra MP, Labrincha JA (2018) Biomass Fly ash geopolymer monoliths for effective methylene blue removal from wastewaters. J Clean Prod 171:783794
13. Marouane E, Saliha A, Mohammed E, Taibi M (2019) Preparation, characterization, and application of Metakaolin-based Geopolymer for removal of methylene blue from aqueous solution. J Chem 2019:1–14. https://doi.org/10.1155/2019/4212901
14. Bai C, Colombo P (2018) Processing, properties and applications of highly porous Geopolymers: a review. Ceram Int 44(14):16103–16118. https://doi.org/10.1016/j.ceramint.2018.05.219
15. Singhal A, Gangwar BP, Gayathry JM (2017) CTAB modified large surface area nanoporous geopolymer with high adsorption capacity for copper ion removal. Appl Clay Sci 150:106–114. https://doi.org/10.1016/j.clay.2017.09.013
16. Sarkar C, Basu JK, Samanta AN (2018) Experimental and kinetic study of fluoride adsorption by Ni and Zn modified LD slag based Geopolymer. Chemical Engineering Research and Design, S0263876218306221–. doi:https://doi.org/10.1016/j.cherd.2018.12.006
17. Runtti H, Luukkonen T, Niskanen M, Tuomikoski S, Kangas T, Tynjälä P, Tolonen E-T, Sarkkinen M, Kemppainen K, Rämö J, Lassi U (2016) Sulphate removal over barium-modified blast-furnace-slag geopolymer. J Hazardous Mater, S0304389416305568. https://doi.org/10.1016/j.jhazmat.2016.06.001
18. Yuanyuan G, Xuemin C, Kong Y, Zhili L, He Y, Qianqian Z (2014) Porous geopolymeric spheres for removal of Cu (II) from aqueous solution: synthesis and evaluation "Ac Ce p Te d Cr T.". Journal of Hazardous Materials (Ii) 283:244–251. https://doi.org/10.1016/j.jhazmat.2014.09.038
19. Y. Liu, C. Yan, Z. Zhang, Y. Gong, H. Wang, and X. Qiu, .(2016). A facile method for preparation of floatable and permeable fly ash-based geopolymer block. Mater Lett 185:370–373 "crossmark," Mater Lett, vol. 185, no. July, pp. 370–373 doi: https://doi.org/10.1016/j.matlet.2016.09.044
20. Sido-Pabyam M, Gueye M, Blin J, Some E (2009) Valorisation de résidus de Biomasse en Charbons actifs – Tests d'efficacité sur des bactéries et dérivés de pesticides. Revue Sud Sciences et Technologies 17:65–73
21. Karadag D (2007) Modeling the Mechanism, Equilibrium and Kinetics for the Adsorption of Acid Orange 8 onto Surfactant-Modified Clinoptilolite. Appl Nonlinear Regression Anal 74:659–664. https://doi.org/10.1016/j.dyepig.2006.04.009
22. Davidovits J (2008) Geopolymer chemistry & applications. Geopolymer Institute, Saint-Quentin
23. Siyal AA, Shamsuddin MR, Khan MI, Rabat E, Zulfiqar M, Man Z, Siame J, Azizli KA (2018) A review on Geopolymers as emerging materials for the. J Environ Manag 224:327–339. https://doi.org/10.1016/j.jenvman.2018.07.046
24. Sangwichien C, Aranovich GL, Donohue MD (2002) Density functional theory predictions of adsorption isotherms with hysteresis loops. Colloids Surf A Physicochem Eng Asp 206:313–320
25. Khan MI, Min TK, Azizli K, Sufian S, Ullah H, Man Z (2015) Effective removal of methylene blue from water using phosphoric acid based geopolymers: synthesis, characterizations and adsorption studies. RSC Adv 5(75):61410–61420. https://doi.org/10.1039/c5ra08255b
26. Tahir SS, Rauf N (2006) Removal of cationic dye from aqueous solutions by adsorption onto bentonite clay. Chemosphere.63, 1842-1848. Ceram Int 44(14):16103–16118. https://doi.org/10.1016/j.ceramint.2018.05.219
27. Panias D, Giannopoulou IP, Perraki T (2007) Effect of synthesis parameters on the mechanical properties of fly ash-based geopolymers. Colloids Surf A Physicochem Eng Asp 301:246–254. https://doi.org/10.1016/j.colsurfa.2006.12.064
28. Maragkos I, Giannopoulou IP, Panias D (2009) Synthesis of Ferronickel Slag-Based Geopolymers. 22:196–203. doi: https://doi.org/10.1016/j.mineng.2008.07.003
29. Rattanasak U, Chindaprasirt P (2009) Influence of NaOH solution on the synthesis of Fly ash Geopolymer. Miner Eng 22(12):1073–1078. https://doi.org/10.1016/j.mineng.2009.03.022
30. Tome S, Etoh M, Etame J, Kumar S (2020) Improved reactivity of volcanic ash using municipal solid incinerator Fly ash for alkali-

activated cement synthesis. Waste and Biomass Valoriz 11(6): 3035–3044. https://doi.org/10.1007/s12649-019-00604-1
31. Tome S, Hermann DT, Shikuku VO, Otieno S (2021) Synthesis, characterization and application of acid and alkaline activated volcanic ash-based geopolymers for adsorptive remotion of cationic and anionic dyes from water. Ceram Int xxx(xxxx):1–9. https://doi.org/10.1016/j.ceramint.2021.04.097
32. Kamseu E, Nait-ali B, Bignozzi MC, Leonelli C, Rossignol S, Smith DS (2012) Bulk composition and microstructure dependence of effective thermal conductivity of porous inorganic polymer cements. J Eur Ceram Soc 32:1593–1603. https://doi.org/10.1016/j.jeurceramsoc.2011.12.030
33. Karim AB, Mounir B, Hachkar M, Bakasse M, Yaacoubi A (2010) Élimination du colorant basique « Bleu de Méthylène » en solution aqueuse par l'argile de Safi. Revue Des Sciences de l'eau 23(4): 375–388. https://doi.org/10.7202/045099ar
34. Dotto GL, Santos JMN, Rodrigues IL, Rosa R, Pavan FA, Lima EC (2015) Adsorption of Methylene Blue by Ultrasonic Surface Modified Chitin. J Colloid Interface Sci. https://doi.org/10.1016/j.jcis.2015.01.046
35. Shikuku VO, Kowenje CO, Kengara FO (2018) Errors in Parameters Estimation Using Linearized Adsorption Isotherms : Sulfadimethoxine Adsorption onto Kaolinite Clay 23(4), 1–6. https://doi.org/10.9734/CSJI/2018/44087
36. Yao C, Chen T (2019) An improved regression method for kinetics of adsorption from aqueous solutions. J Water Process Eng 31(May):100840. https://doi.org/10.1016/j.jwpe.2019.100840
37. McKay G, Otterburn MS, Aga JA (1985) Fuller's earth and fired clay as adsorbents for dyestuffs. Water Air Soil Pollut 24:307–322
38. Ofomaja AE (2008) Sorptive removal of methylene blue from aqueous solution using palm kernel fibre : effect of fibre dose. Biochem Eng J 40:8–18. https://doi.org/10.1016/j.bej.2007.11.028
39. Asseng MC, Dzoujo HT, Dina DDJ, Etoh MA, Tchakounte AN, Nsami JN (2020) Batch Studies for the Removal of a Hazardous Azo Dye Methyl Orange from Water through Adsorption on Regenerated Activated Carbons. J Mater Sci Eng B 10(3):109–123. https://doi.org/10.17265/2161-6221/2020.5-6.003
40. Itodo AU, Itodo HU (2010) Sorption energies estimation using Dubinin Radushkevich and Temkin adsorption isotherms. Life Sci 7:31–39
41. Jia LIU, Wang H-l, Chun-xin LÜ, Han-fei LIU, Zhi-xin GUO, Chun-li K (2013) Water through modified diatomite. Chem Res Chin Univ 29(3):445–448. https://doi.org/10.1007/s40242-013-2504-1
42. Temkin MI, Pyzhev V (1940) Kinetics of ammonia synthesis on promoted iron catalyst, Acta Physiochim. URSS 12:327–356
43. Freundlich H (1906) on adsorption in solution. Z Physik Chem 57: 385–471
44. Sips R (1948) on the structure of a catalyst surface. J Chem Phys 16: 490
45. Anagho S, Tchuifon R, Ndifor-Angwafor G, Ndi J, Ketcha J, Nchare M (2013) Nickel adsorption from aqueous solution onto kaolinite and metakaolinite: kinetic and equilibrium studies. Int J Chem 4:1–7
46. Shikuku VO, Kimosop J (2020) Efficient removal of sulfamethoxazole onto sugarcane bagasse-derived biochar: two and three-parameter isotherms, kinetics and thermodynamics. S Afr J Chem 73:111–119
47. Sarkar C, Basu JK, Samanta AN (2018) Synthesis of mesoporous geopolymeric powder from LD slag as superior adsorbent for zinc (II) removal. Adv Powder Technol, no February: 1–11. https://doi.org/10.1016/j.apt.2018.02.005
48. Maragkos I, Giannopoulou IP, Panias D (2009) Synthesis of ferronickel slag-based geopolymers. Miner Eng 22:196–203. https://doi.org/10.1016/j.mineng.2008.07.003